Journal of Atmospheric and Solar-Terrestrial Physics 73 (2011) 77–87

Contents lists available at ScienceDirect

Journal of Atmospheric and Solar-Terrestrial Physics

journal homepage: www.elsevier.com/locate/jastp

Solar cycle variations of outer radiation belt and its relationship to solar wind structure dependences

Y. Miyoshi [a,*], R. Kataoka [b]

[a] Solar-Terrestrial Environment Laboratory, Nagoya University, Japan
[b] Tokyo Institute of Technology, Japan

ARTICLE INFO

Article history:
Received 15 June 2009
Received in revised form
19 June 2010
Accepted 28 September 2010
Available online 13 October 2010

Keywords:
Radiation belts
Solar wind structures
Solar cycle variations
Space weather

ABSTRACT

The outer radiation belt shows solar cycle variation: the L-shell of the electron flux peak in the outer belt shifts inward during the period between the rising phase and the solar maximum, while it shifts outward between the beginning of the declining phase and the solar minimum. We show a possible mechanism which considers two typical types of magnetic storms categorized in accordance with solar wind drivers, namely coronal mass ejections (CMEs) and corotating interaction regions (CIRs). Large flux enhancements at the inner portion of the outer belt tend to occur during the recovery phase of great storms driven by CMEs, while large flux enhancements at the outer portion and at geosynchronous orbit tend to occur during the recovery phase of relatively moderate storms driven by CIRs. High-speed coronal hole streams which do not always cause large magnetic storms also effectively enhance the electron flux enhancement at the outer portion and in geosynchronous orbit. In this framework, the plasmapause always plays an important role in both flux enhancement and flux loss in the outer belt. The average plasmapause position depends on the storm amplitude, and the plasmapause reaches closest to the Earth during great storms driven by CMEs. CMEs themselves and CME-driven storms occur during maximum periods of solar activity, while CIRs themselves and CIR-driven storms occur during the solar declining phase. The observed long-term variations of the outer belt can therefore be understood in terms of their dependence on the large-scale interplanetary structures, varying depending on the phase of the solar cycle.

1. Introduction

The Van Allen radiation belts (Van Allen and Frank, 1959) consist of relativistic electrons and ions which are trapped in the terrestrial magnetic field and move under the influence of electric and magnetic fields in the inner magnetosphere. There are two regions of the electron radiation belts, namely the inner belt at around 1.5 Re and the outer belt at around 4–7 Re. Understanding and forecasting the flux enhancement of the outer belt electrons is a key topic in space weather research since large fluxes of relativistic electrons can cause damage to satellites and other important services for modern life (Baker et al., 1987, 1998a; Lanzerotti, 2001; Pilipenko et al., 2006).

Among the multi-scale temporal variation of the outer radiation belt (Baker et al., 1999; Li et al., 2001; Miyoshi et al., 2004), the most violent variations occur during magnetic storms. The time scale of storms is of the order of several days. The outer belt electron flux typically decreases during the storm main phase, and then the flux recovers to and often increases over the pre-storm level (Baker et al., 1986; Nagai, 1988; Reeves et al., 2003). The large flux enhancement depends on the storm driver source such as coronal mass ejections (CMEs) and corotating interaction regions (CIRs) (Miyoshi and Kataoka, 2005; Kataoka and Miyoshi, 2006): CIR-driven storms tend to enhance the flux at the outer portion of the outer belt, while CME-driven great storms (average Dst < -150 nT) tend to enhance the flux at the inner portion of the outer belt and in the slot region (Miyoshi and Kataoka, 2005).

Semi-annual variations of the outer belt are also clearly observed, which the electron flux largely increases in spring and fall (Baker et al., 1999, 2004a; Li et al., 2001; Miyoshi et al., 2004; Baker and Kanekal, 2008). A possible explanation for the origin of these semi-annual variations is that of geomagnetic activity (Baker et al., 1999; Baker and Kanekal, 2008). Since relativistic electron flux enhancements in the outer belt are sensitive to the southward component of the interplanetary magnetic field (IMF), and the spring-toward fall-away (STFA) rule of the Russell–McPherron effect (Russell and McPherron, 1973) produces considerable southward IMF, the electron flux tends to increase in spring and fall (McPherron and Weygand, 2006; Miyoshi and Kataoka, 2008a, b; McPherron et al., 2009).

Solar cycle variations of the outer belt also exist (Belian et al., 1996; Miyoshi et al., 2004; Li et al., 2006; Fung et al., 2006; Baker and Kanekal, 2008), consisting the highest hierarchy of the multi-scale

---

[*] Corresponding author. Tel.: +81 52 747 6340.
E-mail address: miyoshi@stelab.nagoya-u.ac.jp (Y. Miyoshi).

1364-6826/$ - see front matter © 2010 Elsevier Ltd. All rights reserved.
doi:10.1016/j.jastp.2010.09.031

temporal variation. Fung et al. (2006) suggested that solar cycle variation of ionospheric density scale heights cause solar cycle variations of the position of the slot region since the resonance condition of the pitch angle scattering with whistler mode waves is sensitive to the ratio of the electron plasma frequency and the gyro frequency. The occurrence of CME- and CIR-driven storms depends on the phase of the solar cycle (e.g., Kataoka and Miyoshi, 2006; Richardson et al., 2006; Zhang et al., 2006; Baker and Kanekal, 2008), and there are many differences in magnetospheric responses between CME- and CIR-driven storms (e.g., Borovsky and Denton, 2006; Denton et al., 2006; Tsurutani et al., 2006a).

It has been expected that the long-term occurrence of the storm driver sources affect the flux variations and the outer belt structures (e.g., Baker et al., 2004a; Miyoshi and Kataoka, 2005, 2008a, b; Baker and Kanekal, 2008). In our previous papers, we have studied the solar wind structure dependences of the outer radiation belt (Miyoshi and Kataoka, 2005; Kataoka and Miyoshi, 2006; Miyoshi and Kataoka, 2008a, b), and discussed the possible acceleration mechanisms (Miyoshi et al., 2007). However, it has never been discussed how large-scale storm drivers CMEs and CIRs as well as high-speed streams affect the solar cycle variations of the outer belt, and it is necessary to study solar cycle variations based on the average profiles of the outer belt for different solar wind structures such as CMEs and CIRs. In this paper, we discuss the solar cycle variations, based on the characteristics of the outer radiation belt in response to different solar wind conditions/structures, and the possible acceleration mechanisms behind the solar cycle variation.

2. Data

As a uniform data set of the radiation belt electrons for solar cycles, we used energetic electron observations at a wide range of L-shells obtained from the MEPED instrument onboard the NOAA/POES satellites (POES-6, 8, 10, 12 and 15) between July 1979 and December 2008. The altitude of POES-6, 8 and 12 was 815.5 km, and that of POES-10 and 15 was 830.0 km. We show the data from the local trapped electron detector (so-called 90° sensor) of >300 keV. Details of the instruments on board satellites up to POES-12 are described by Raben et al. (1995), and those on POES-15 are described by Evans and Greer (2000). In the analysis, we selected only the data for the Northern Hemisphere in order to avoid the effects of the South Atlantic Anomaly, and used 1-day averaged data. At low latitude, the sensor on board POES-15 measures particles in the local atmospheric loss cone, while the pitch angle measured by previous POES satellites at the same location is close to 90°. For this reason, the count rates at low latitude observed by POES-15 are extremely low, and therefore we do not discuss the electron flux on NOAA 15 below $L<2.5$. Note that the L-shell used in this study is McIlwain L, as determined from the DGRF/IGRF model. In addition to the low-altitude POES data, we used the >2 MeV electron data from GOES satellites at geosynchronous orbit for solar cycle 23. The 27-day averaged solar wind data are obtained from the OMNI-2.

3. Data analysis

Fig. 1 shows the L–time diagram for 300 keV electrons, the L-shell of the flux peak in the outer belt, and the sunspot number for the period between 1979 and 2008. Large flux enhancements at the inner portion of the outer belt ($L<4.5$) are observed around the solar maximum and the early declining phase, while the flux at the outer portion of the outer belt ($L>4.5$) remains at usual or low level during this period. On the other hand, large fluxes tend to be observed at the outer region of the outer belt ($L>4.5$) during the

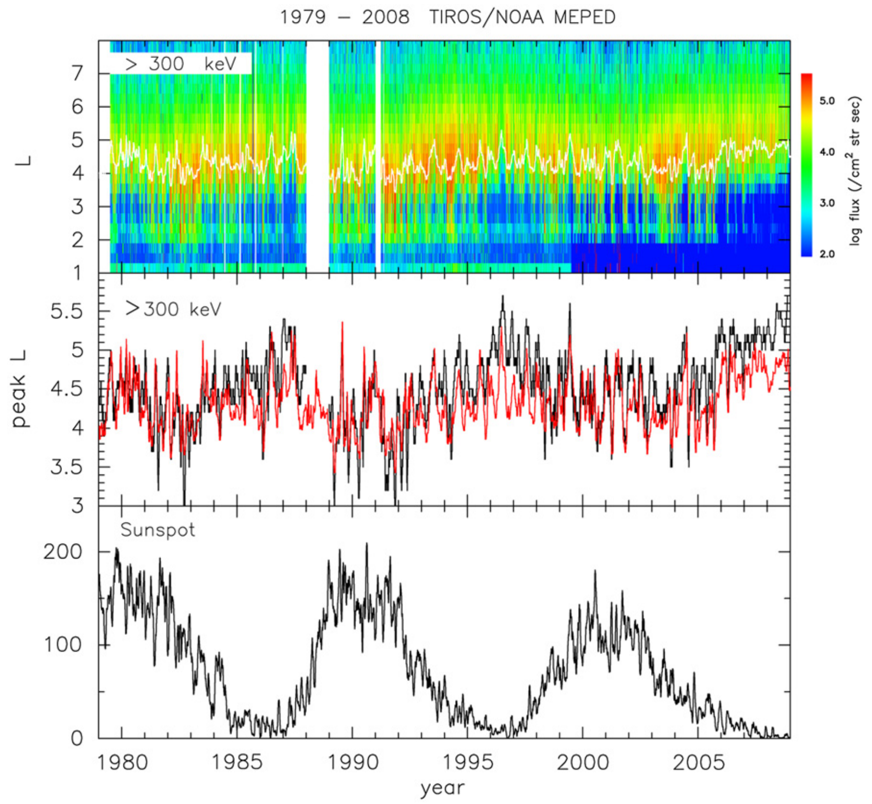

Fig. 1. (a) L–time diagram of >300 keV electrons for the period between 1979 and 2008. (b) The L-shell of >300 keV electron flux peak. Superimposed white (a) and red (b) lines show the minimum of the plasmapause for every 10 days from the empirical model and (c) number of sunspots.